A Detailed Procedure to Implement Model Predictive Control for the Single-Phase Voltage-Source Inverter

Dung H. Vu, Son T. Nguyen*, Tu M. Pham, Anh Hoang

Hanoi University of Science and Technology, Vietnam
**Corresponding author E-mail: son.nguyenthanh@hust.edu.vn*

Abstract

This study aims to provide a detailed procedure to deploy model predictive control (MPC) for the single-phase voltage-source inverter. Simulation and implementation of other control methods for the single-phase voltage-source inverter, including the sinusoidal pulse width (SPWM) and the hysteresis methods, are also given. In MPC control deployment for the single-phase voltage-source inverter, the mathematical model of the inverter is first required. Based on the obtained model of the inverter, discrete-time forms of the inductor current and the capacitor voltage can be conveniently formulated. The optimal control action in each sampling interval is selected based on the minimum value of a cost function, defined as the difference between the predicted value and the desired value of the current or voltage. Compared to conventional control methods for the single-phase inverter, the MPC method requires accurate sensors, and its implementation is also sometimes challenging. In this study, control methods for the single-phase voltage-source inverter are conveniently deployed using the KIT STM32F407 DISCOVERY. The simulation and experimental results have proven that the MPC algorithm is suitable for fully understanding the concept of model-based discrete control of the single-phase voltage-source inverter and other types of power converters.

***Keywords**: Single-phase inverter, model predictive control, the KIT STM32F407 DISCOVERY.*

Symbols

Symbols	Units	Description
V_{DC}	V	DC source voltage
V_{AB}	V	Output voltage of the inverter
L	H	Inductance of the inductor
C	µF	Capacitance of the capacitor
T_s	second	Sampling interval
$i_L(k)$	A	Inductor current at the k-th sampling instant
$i_L(k-1)$	A	Inductor current at the $k-1$-th sampling instant
$i_L(k+1)$	A	Inductor current at the $k+1$-th sampling instant
$v_C(k)$	V	Load voltage at the k-th sampling instant
$v_C(k-1)$	V	Load voltage at the $k-1$-th sampling instant
$v_C(k+1)$	V	Load voltage at the $k+1$-th sampling instant

Abbreviations

MPC	Model predictive control
UPS	Uninterruptible power supply
THD	Total harmonic distortion
RMS	Root-Mean-Square
SPWM	Sinusoidal pulse width modulation
FCS-MPC	Finite Control Set MPC
GUI	Graphical user interface
DAQ	Data acquisition
PI	Proportional-Integral

Tóm tắt

Nghiên cứu này nhằm mục đích cung cấp một quy trình chi tiết để triển khai điều khiển dự đoán mô hình (MPC) cho bộ nghịch lưu nguồn áp một pha. Mô phỏng và triển khai các phương pháp điều khiển khác cho bộ nghịch lưu nguồn áp một pha bao gồm phương pháp điều chế độ rộng xung hình sin (SPWM) và phương pháp trễ cũng được đề cập trong nghiên cứu này. Trong quá trình triển khai điều khiển MPC cho bộ nghịch lưu nguồn áp một pha, trước tiên cần có mô hình toán học của bộ nghịch lưu. Dựa trên mô hình thu được của bộ nghịch lưu, dạng thời gian rời rạc của dòng điện qua cuộn cảm và điện áp trên tụ điện có thể được xây dựng một cách thuận tiện. Hành động điều khiển tối ưu trong mỗi khoảng thời gian lấy mẫu được lựa chọn dựa trên giá trị nhỏ nhất của hàm chi phí được định nghĩa là sự khác biệt giữa giá trị dự báo và giá trị mong muốn của dòng điện qua cuộn cảm hoặc điện áp trên tụ điện. So với các phương pháp điều khiển thông thường cho bộ nghịch lưu nguồn áp một pha, phương pháp MPC yêu cầu các cảm biến chính xác và việc triển khai phương pháp này đôi khi cũng gặp nhiều thách thức. Trong nghiên cứu này, các phương pháp điều khiển cho bộ nghịch lưu nguồn áp một pha được triển khai thuận tiện bằng cách sử dụng KIT STM32F407 DISCOVERY. Kết quả mô phỏng và thực nghiệm đã chứng minh rằng thuật toán MPC phù hợp để hiểu đầy đủ khái niệm điều khiển rời rạc dựa trên mô hình của bộ nghịch lưu nguồn áp một pha cũng như các loại bộ biến đổi công suất khác.

1. Introduction

Power converters have been in continuous development since the second half of the 20th century. Power converter control methods have also become interesting topics in the field of power electronics. The single-phase voltage-source inverter is ideally used in single-phase power supplies such as single-phase uninterruptible power supply (UPS) applications, and single-phase grid-connected systems [1-5]. Meanwhile, the three-phase voltage-source inverter is mostly used in variable frequency drives, three-phase UPS devices and flexible AC

Received: 9 November 2024; Accepted: 16 December 2024.

transmission systems. With recent advanced control technologies in power electronics, UPS systems are required to have an output voltage with very low total harmonic distortion (THD). According to the IEEE 547 standard, the minimum THD in the output voltage of UPS systems must be maintained to be lower than 5% [1] for nonlinear loads.

The current-controlled single-phase inverters are more popular than the voltage-controlled single-phase inverters. The current-controlled single-phase inverters can be used in grid-connected systems. The control of the single-phase inverter's output current can be classified into linear and nonlinear techniques. In linear control methods, the output current of the inverter can be controlled using a conventional PI controller with the use of the sinusoidal pulse width modulation (SPWM) technique [6,7], Nonlinear control strategies include dead-beat control [8], hysteresis control [9], iterative learning control [10] and sliding mode control [11].

The dead-beat control belongs in the family of predictive regulators. If the dead-beat controller can be suitably tuned, it can have a fast response with a very small tracking error. However, the dead-beat controller tends to have uncertainties, data mismatch and noise at a high sampling frequency. The hysteresis control method is used to compare the output current to the reference current to generate switching signals for the inverter. The main advantage of this control method is its simplicity in implementation.

Model predictive control (MPC) has recently emerged as an effective control method for various power electronic converters because it can deal with non-linearities of the system and obtain a fast dynamic response. In the MPC method, the discrete-time model of the system is considered to predict the future behaviors of the variables over a time frame [12-17]. These predictions are performed by using a cost function which is simply defined as the error between the desired controlled variable and the measured value.

MPC has several advantages over other control techniques, such as its ability to handle complex and uncertain systems. It can also consider constraints in a defined cost function. In addition, MPC can incorporate feedback and feedforward information, as well as external signals or references, to improve tracking and disturbance rejection. MPC is also easily tuned and modified by changing the parameters of the cost function or the constraints.

Implementation of the MPC for power converters can be done by taking advantage of the inherent discrete nature of power converters. Since power converters only have a finite number of switching states, the MPC application can be significantly simplified and reduced to the prediction of the system behaviors for possible switching states of the power converter. This approach is also known as Finite Control Set MPC (FCS-MPC) for power converters.

The pulse control for voltage modulation can be performed by FCS-MPC with the following items:

- Defining a finite set of voltage states: a finite set of possible voltage states is defined. Each state corresponds to a specific configuration of the switching devices in the power converter.
- Predicting future behaviour: At each control step, the future trajectory of the output voltage or current over a finite prediction horizon using the system model and the chosen switching states
- Optimization: An optimization problem is solved to select the switching sequence that minimizes the deviation between the predicted output and the desired output. This optimization is based on an objective function, which typically includes tracking error (the difference between the predicted and desired voltage or current) and may also include other factors like minimizing switching losses or ensuring system stability.
- Discrete switching decision: Since the switching states are discrete, the optimization considers only those switching combinations that are available in the finite set. These are usually based on predefined voltage vectors.
- Feedback: After the control decision is made, the switches are set to a new state, and the output voltage or current is measured. The control loop then repeats at the next sampling instant, where the algorithm takes the updated system state into account.

The FCS-MPC can be utilized to effectively control the output current of single-phase voltage-source inverters with low total harmonic distortion (THD) and noise. However, the practical implementation of the FCS-MPC is usually challenging. Therefore, in this study, a general FCS-MPC approach for controlling the output current of the single-phase voltage-source inverter is described in detail with the inclusion of theory, simulation, and implementation.

The contribution of this study is to describe clear steps to implement the MPC for the single-phase voltage-source inverter. This work has usually been mentioned briefly in many publications. The hardware used in this study, the KIT STM32F407 DISCOVERY, has a very reasonable price and it can be utilized to quickly deploy complicated control algorithms with the effective support of MATLAB Simulink. The library to program the KIT STM32F407 DISCOVERY in MATLAB Simulink is free and downloadable from the web [18]. These are very valuable in studying the advanced control methods of power converters both in theory and implementation.

The study also gives a comparison between other control methods and the FCS-MPC method of the current-controlled single-phase inverter. According to the experimental results obtained, the performance of the single-phase inverter controlled by using the FCS-MPC method can outperform the performance of the inverter controlled by other control methods in the reduction of the inductor current's harmonics.

This study first mentions three control algorithms for the output current of the single-phase voltage-source inverter including the SPWM, hysteresis and MPC methods. Next, the load voltage control of the voltage-controlled single-phase inverter is presented. The paper is organized as follows. Section 2 provides the concept of MPC for controlling the inductor current of the current-controlled inverter and the voltage across the capacitor of the voltage-controlled single-phase inverter. Simulation tasks of MPC for the inverter are

presented in Section 3. Details of the implementation of different control strategies for the inverter are described in Section 4. Finally, Section 5 is the conclusion and future research direction for this topic.

2. Model Predictive Control of the Single-Phase Voltage-Source Inverter

2.1. Current Predictive Control of the Single-Phase Inverter

Figure 1 shows the topology of the single-phase voltage-source inverter. The load has the inductive property with the resistance R and inductance L. The inverter has four semiconductor switches S_1, S_2, S_3 and S_4. Switching states of two switches in the same leg are opposite each other. This means that if S_1 is switched on, then S_3 is switched off and vice versa. Similarly, if S_2 is switched on, then S_4 is switched off and vice versa.

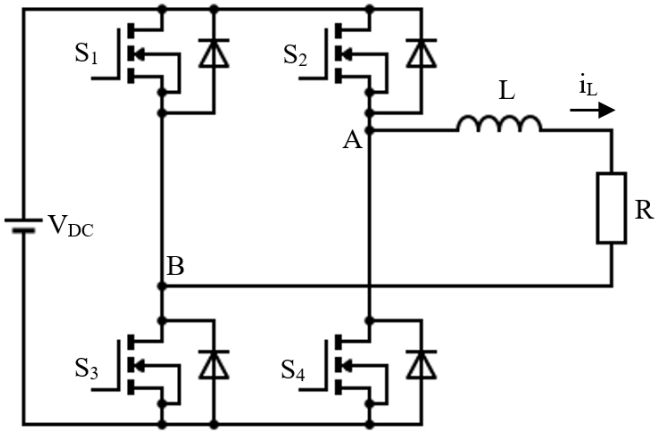

Figure 1: Single-phase voltage-source inverter.

The output voltage of the inverter V_{AB} is determined as follows:

$$V_{AB} = V_{DC}\left(S_A - S_B\right) \tag{1}$$

In which

- V_{DC} is the DC source voltage.
- S_A and S_B are binary control variables having the following properties:
  - If $S_A = 1$, then S_2 is switched on and S_4 is switched off.
  - If $S_A = 0$, then S_2 is switched off and S_4 is switched on.
  - If $S_B = 1$, then S_1 is switched on and S_3 is switched off.
  - If $S_B = 0$, then S_1 is switched off and S_3 is switched on.

The voltage equation of the inverter is as follows:

$$V_{AB} = L\frac{di_L}{dt} + Ri_L \tag{2}$$

$$\frac{di_L}{dt} \approx \frac{i_L(k) - i_L(k-1)}{T_s} \tag{3}$$

The discrete-time form of equation (2) is given by:

$$V_{AB}(k) = L\frac{i_L(k) - i_L(k-1)}{T_s} + Ri_L(k) \tag{4}$$

In which

- $i_L(k)$ is the inductor current at the k-th sampling instant.
- $i_L(k-1)$ is the inductor current at the $k-1$-th sampling instant.
- $V_{AB}(k)$ is the output voltage of the inverter at the k-th sampling instant.
- T_s is the sampling interval.

Re-arranging equation (4) results in:

$$i_L(k) = \frac{T_s}{L + RT_s}V_{AB}(k) + \frac{L}{L + RT}i_L(k-1) \tag{5}$$

Moving one-step ahead for equation (5) gives:

$$i_L(k+1) = \frac{T_s}{L + RT_s}V_{AB}(k+1) + \frac{L}{L + RT_s}i_L(k) \tag{6}$$

In equation (6), the current $i_L(k+1)$ is called the predictive or future current at the $k+1$-th sampling instant. $V_{AB}(k+1)$ is computed using (1). The predictive current control of the inverter requires pre-determined values of V_{DC}, R and L.

The optimal control of the output current of the inverter is equivalent to minimizing a cost function simply defined as follows:

$$S = \left|i_L^* - i_L(k+1)\right| \tag{7}$$

In which $i^*(k+1)$ is the reference current at the $(k+1)$-th sampling instant. Figure 2 shows a flowchart of the predictive control of the load current.

$$S = \left|i_L^* - i_L(k+1)\right| + w\sum_{i=1}^{4}\left[S_i(k) - S_i(k-1)\right] \tag{8}$$

where w is known as the weighting factor. $S_i(k)$ and $S_i(k-1)$ is the switching state of the i-th switch at the k-th and the $(k-1)$-th sampling intervals, respectively. A flowchart of the predictive control of the load current is described in Figure 2.

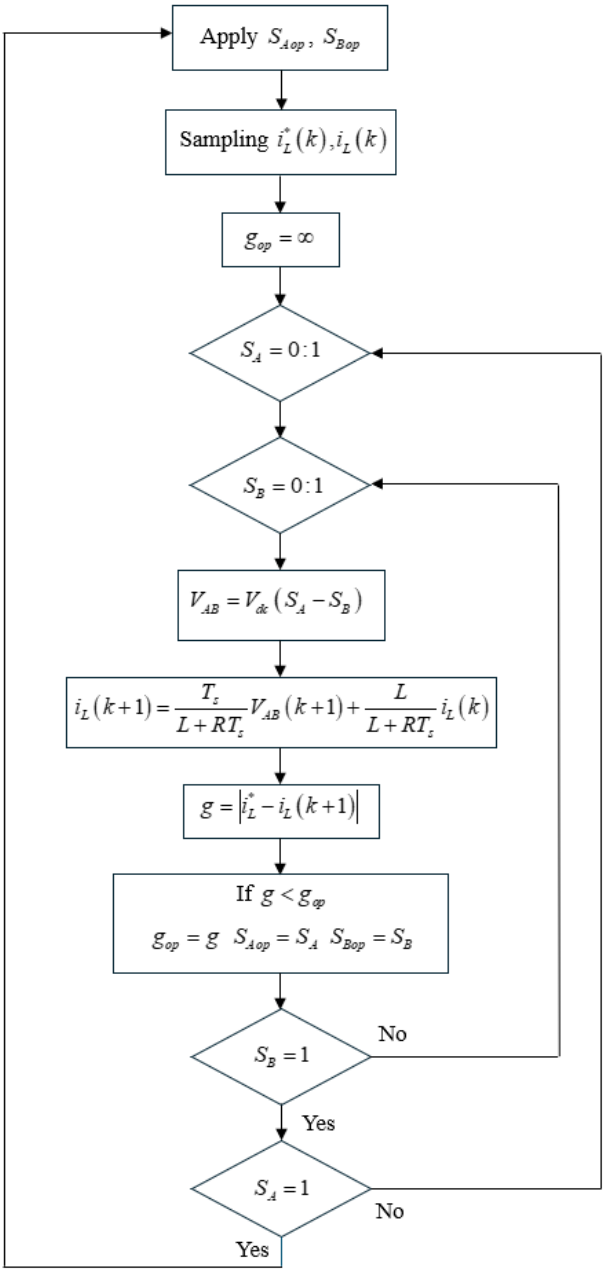

Figure 2: Flowchart of the predictive control of the load current.

2.2. Voltage Predictive Control of the Single-Phase Inverter

The topology of the single-phase voltage-source inverter for UPS applications is shown in Figure 3. The conventional method for controlling the load voltage is related to the design of two control loops: an inner current loop and an external voltage loop as shown in Figure 4.

There are different choices for several controlled parameters using the internal current loop such as the filter capacitor current, inductor current and load current. After designing the inner current loop, the voltage controller needs to be designed such that all kinds of loads are fed with a fixed sinusoidal voltage. The sinusoidal pulse width modulation (SPWM) can be seen as the well-known technique to keep the sinusoidal waveform for the load voltage.

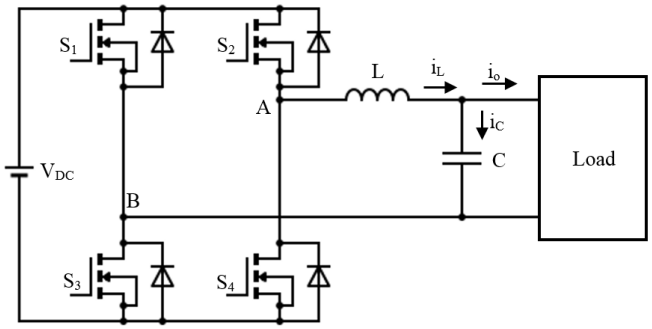

Figure 3: Single-phase UPS.

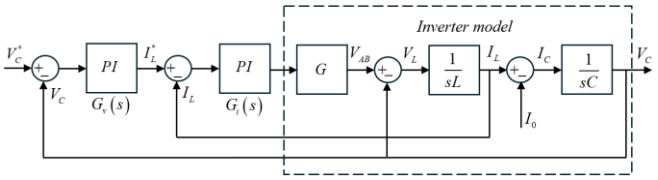

Figure 4: Block diagram of the single-phase voltage-source inverter with two control loops.

where

- V_C^* is the reference voltage
- V_C is the measured voltage
- I_L^* is the reference current through the inductor
- I_L is the measured current through the inductor
- L is the inductance of the inductor
- C is the capacitance of the capacitor
- I_0 is the load current
- G is the inverter gain
- V_{AB} is the output voltage of the inverter
- $G_i(s)$ is the transfer function of the current controller
- $G_v(s)$ is the transfer function of the voltage controller

The output voltage of the inverter is given by:

$$v_{AB} = V_{dc}(S_A - S_B) \tag{9}$$

The inductor current is expressed as follows:

$$L\frac{di_L}{dt} = v_{AB} - v_C \tag{10}$$

The derivative in (10) can be approximated with a sample time T_s at the k-th sampling interval as follows:

$$L\frac{i_L(k) - i_L(k-1)}{T_s} = v_{AB}(k) - v_C(k) \tag{11}$$

Re-arranging (11) gives:

$$i_L(k) = i_L(k-1) + \frac{T_s}{L}\left[v_{AB}(k) - v_C(k)\right] \tag{12}$$

Moving one-step ahead for equation (12) results in:

$$i_L(k+1) = i_L(k) + \frac{T_s}{L}\left[v_{AB}(k+1) - v_C(k+1)\right] \tag{13}$$

If v_C is continuous and T_s is small enough, then $v_C(k+1) \approx v_C(k)$. $v_{AB}(k+1)$ is still determined according to (9). Equation (13) yields:

$$i_L(k+1) = i_L(k) + \frac{T_s}{L}\left[v_{AB}(k+1) - v_C(k)\right] \tag{14}$$

The voltage across the capacitor (the load voltage) is given by:

$$C\frac{dv_C}{dt} = i_L - i_0 \tag{15}$$

The derivative in (15) can be approximated with a sample time T_s at the k-th sampling interval as follows:

$$C\frac{v_C(k)-v_C(k-1)}{T_s} = i_L(k)-i_0(k) \tag{16}$$

Re-arranging (16) results in:

$$i_0(k) = i_L(k) - \frac{C}{T_s}\left[v_C(k)-v_C(k-1)\right] \tag{17}$$

Re-arranging (16) results in:

$$v_C(k) = v_C(k-1) + \frac{T_s}{C}\left(i_L(k)-i_0(k)\right) \tag{18}$$

Moving one-step ahead for equation (18) results in:

$$v_C(k+1) = v_C(k) + \frac{T_s}{C}\left(i_L(k+1)-i_0(k+1)\right) \tag{19}$$

If i_0 is continuous and T_s is small enough, then $i_0(k+1) \approx i_0(k)$ and equation (19) yields:

$$v_C(k+1) = v_C(k) + \frac{T_s}{C}\left(i_L(k+1)-i_0(k)\right) \tag{20}$$

In (20), the load voltage can be estimated as follows:

$$i_0(k) = i_L(k) + \frac{C}{T_s}\left[V_C(k)-V_C(k-1)\right] \tag{21}$$

Finally, the optimal control of the load voltage is equivalent to minimizing a cost function is defined as follows:

$$S = \left|v_C^* - v_C(k+1)\right| \tag{22}$$

In which $v_C^*(k+1)$ is the $(k+1)$-th reference load voltage. In some cases, the cost function should be defined with the inclusion of the frequency constraints as follows:

$$S = \left|v_C^* - v_C(k+1)\right| + w\sum_{i=1}^{4}\left[S_i(k)-S_i(k-1)\right] \tag{23}$$

The flowchart of the predictive control of the load voltage is shown in Figure 5.

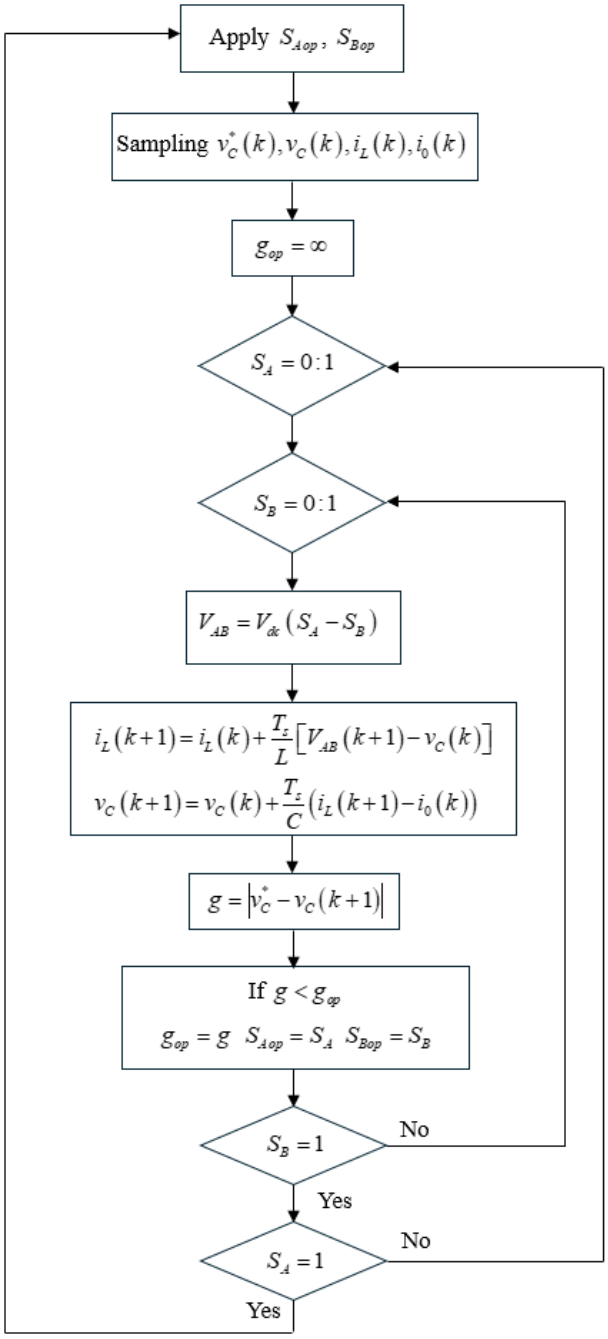

Figure 5: Flowchart of the predictive control of the load voltage.

3. Simulation

3.1. Current Control Using the SPWM Method

Figure 6 shows a Simulink-based simulation diagram of the load current control of the single-phase voltage-source inverter using the SPWM method. The output of the inverter provides power to a load formed by an inductor of 0.6667 H connected in series with a resistor of 210 Ω.

The SPWM method requires a comparison of a modulation wave and a carrier wave. The modulation wave is a 50Hz sine wave and the triangle carrier wave has a frequency of 50 times the modulation wave's frequency. A proportional-integral (PI) controller is responsible for maintaining the desired value of the inductor current. The controller has a proportional gain of 100 and an integral gain of 1. The RMS value of the desired load current is 0.5 (A). Figure 7 shows waveform and FFT analysis of the load current.

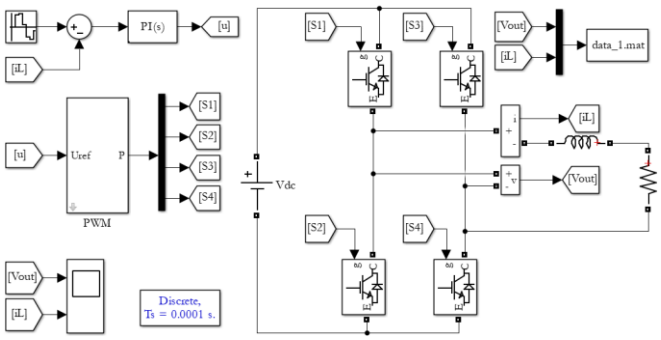

Figure 6: Simulink-based simulation diagram of the load current control of the inverter using the SPWM method.

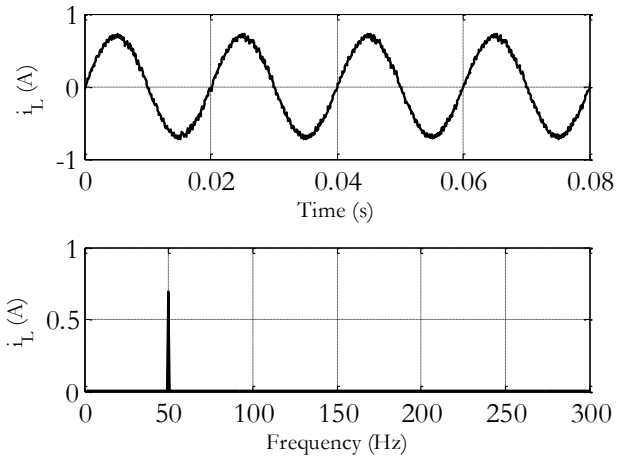

Figure 7: Waveform and FFT analysis of the load current (the SPWM method).

3.2. Current Control Using the Hysteresis Method

Figure 8 shows a Simulink-based simulation diagram of the load current control of the single-phase voltage-source inverter using the hysteresis method. A PI controller is responsible for maintaining the desired value of the current. The controller has a proportional gain of 100 and an integral gain of 1. The RMS value of the desired current is 0.5 (A). Figure 9 shows waveform and FFT analysis of the load current.

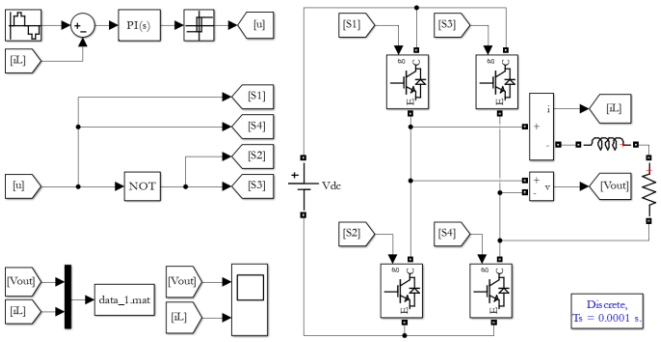

Figure 8: Simulink-based simulation diagram of the load current of the inverter using the hysteresis method.

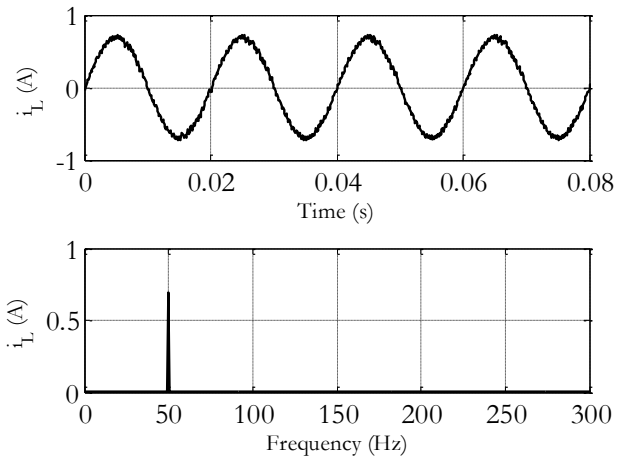

Figure 9: Waveforms and FFT analysis of the load current (the hysteresis method).

3.3. Current Control Using the MPC Method

Figure 10 shows a Simulink-based simulation diagram of the predictive load current control of the single-phase voltage-source inverter using the MPC. The RMS value of the desired current is 0.5 (A). Figure 11 shows waveform and FFT analysis of the load current.

Table 1 indicates total harmonic distortion (THD) of the load current corresponding to three control methods. The MPC method can result in the lowest value of the THD.

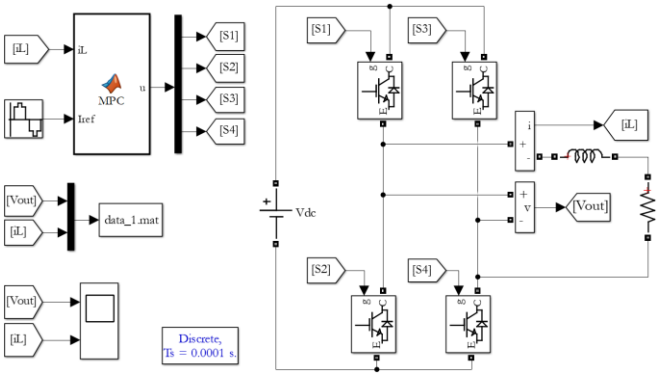

Figure 10: Simulink-based simulation diagram of the load current control of the inverter using the MPC method.

A MATLAB function of the MPC controller in Simulink has the following form:

```
function u = MPC(iL,Iref)
R = 210;
L = 0.66667;
Vdc = 260;
Ts = 1e-5;
Sa_opt = 0;
Sb_opt = 0;
g_opt = inf;
for Sa = 0:1
   for Sb = 0:1
      Vab = Vdc*(Sa - Sb);
      iL_1 = Ts/(L + R*Ts)*Vab + L/(L + R*Ts)*iL;
      g = abs(Iref - iL_1);
      if (g < g_opt)
         Sa_opt = Sa;
         Sb_opt = Sb;
         g_opt = g;
      end
   end
end
Sa = Sa_opt;
Sb = Sb_opt;
u = [Sa; not(Sa); Sb; not(Sb)];
```

Table 1: THD of the load current corresponding to three control methods.

Control Method	THD (%)
SPWM	2.2172
Hysteresis	1.6733
MPC	1.5649

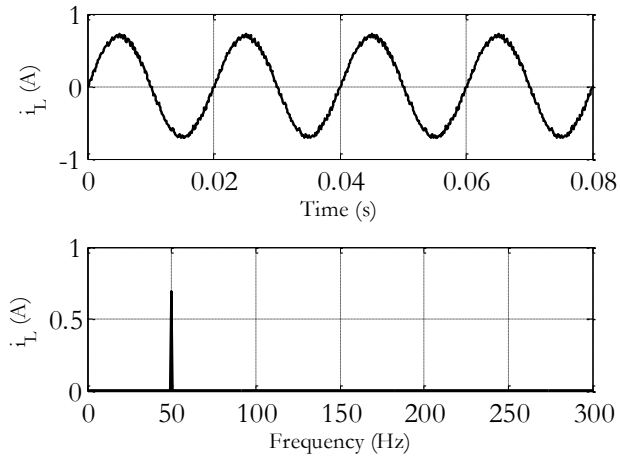

Figure 11: Waveform and FFT analysis of the load current (the MPC method).

3.4. Voltage Control Using the MPC Method

Figure 12 shows a Simulink-based simulation diagram of the load voltage control of the single-phase voltage-source inverter using the MPC method. The desired RMS value of the sinusoidal load voltage is 100 (V). Figure 13 shows waveforms of the inductor current and load voltage.

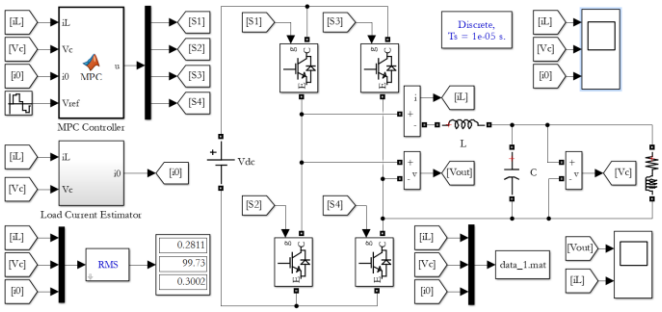

Figure 12: Simulink-based simulation diagram of predictive capacitor voltage control.

MATLAB function of the MPC controller in Simulink has the following form:

```
function u = MPC(iL,Vc,i0,Vref)
L = 0.6667;
C = 8e-6;
Vdc = 260;
Ts = 1e-4;
Sa_opt = 0;
Sb_opt = 0;
g_opt = inf;
for Sa = 0:1
   for Sb = 0:1
      Vab = Vdc*(Sa - Sb);
      iL_1 = iL + Ts/L*(Vab - Vc);
      Vc_1 = Vc + Ts/C*(iL_1 - i0);
      g = (Vref - Vc_1)^2;
      if (g < g_opt)
         Sa_opt = Sa;
         Sb_opt = Sb;
         g_opt = g;
      end
   end
end
Sa = Sa_opt;
Sb = Sb_opt;
u = [Sa; not(Sa); Sb; not(Sb)];
```

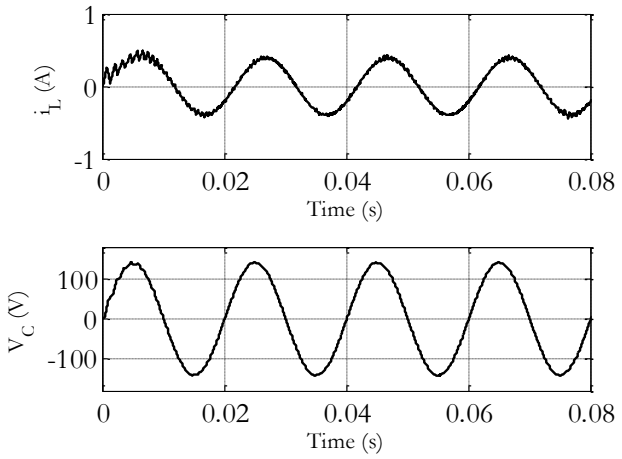

Figure 13: Waveforms of the inductor current and load voltage.

4. Experiment

To consolidate the effectiveness of the FCS-MPC method for the single-phase voltage-source inverter, the following experiments were carried out:

- The inductor current in the current-controlled inverter was controlled using the SPWM method, the hysteresis method and the FCS-MPC method.
- The capacitor voltage in the voltage-controlled was controlled using the FCS-MPC method.

An experimental system shown in Figure 14 was established with the following components:

- A DC voltage source.
- A single-phase H bridge.
- A resistive-inductive load.
- Voltage and current isolators
- Voltage and current sensors.
- A KIT STM32F407 DISCOVERY.
- A NI-USB 6009 data acquisition device.
- A laptop with a graphical user interface (GUI) software for data acquisition, as shown in Figure 15.

The voltage isolator can work with the input voltage ranging from 0 to +/-600V corresponding to the output voltage ranging from 0 to +/-10V. The current isolator can work with the input current ranging from 0 to +/-5A corresponding to the output voltage ranging from 0 to +/-10V. The signals from the output voltages of the voltage and current isolators are required to be further processed to obtain the DC voltage accepted for the range of the ADC inputs of the KIT STM32F407 DISCOVERY.

The graphical user interface (GUI) software was written using the LabVIEW software to display real-time waveforms and rms values of the output voltage of the inverter and the inductor current. These waveforms were recorded in data files to re-plot using the MATLAB software for an off-line analysis of harmonic distortion of the inductor current.

The KIT STM32F407 DISCOVERY, based on the STM32F407 microcontroller, allows its users to conveniently develop control algorithms. It is produced with a trade-off between the high performance and expense of its. The KIT STM32F407 DISCOVERY can be programmed using either

C programming language or MATLAB Simulink. In this study, MATLAB Simulink was used to develop control algorithms for the single-phase voltage-source inverter. In particular, the Waijung Blockset, a free and downloadable MATLAB Simulink library for the KIT STM32F407 DISCOVERY, is used to deploy control algorithms for the inverter [18].

The Waijung Blockset allows users to program the control algorithm using MATLAB Simulink. In addition, the user can use the Build Model to directly transfer the proposed control algorithm from the Simulink environment to the KIT STM32F407 DISCOVERY.

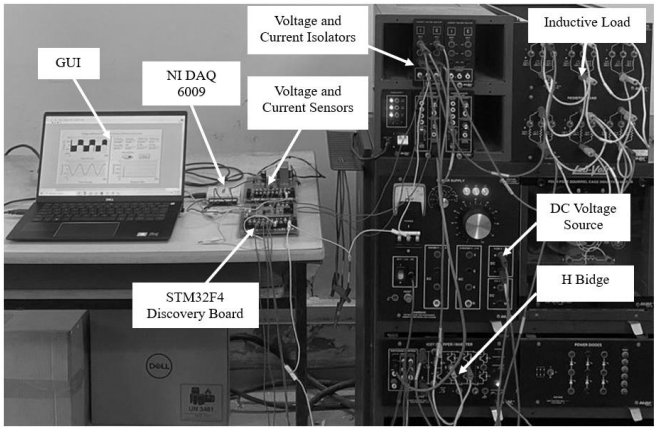

Figure 14: The experimental system.

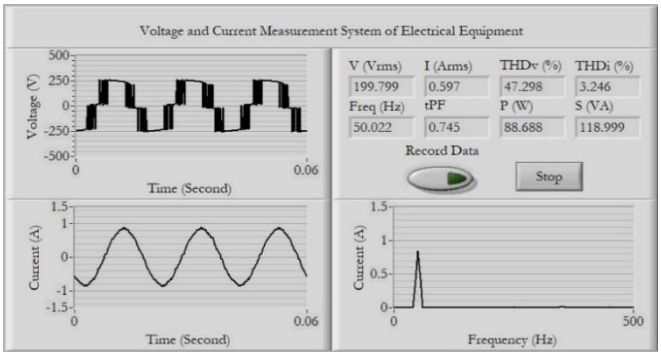

Figure 15: GUI of the software for data acquisition.

4.1. Current Control Using the SPWM Method

Figure 16 is a Simulink-based diagram to deploy the SPWM control method on the KIT STM32F407 DISCOVERY. The control method requires the measurement of the inductor current with a Proportional-Integral (PI) controller. Waveform and RMS value of the inductor current were also acquired using the NI-6009 DAQ device for an offline analysis using MATLAB. Figure 17 is waveform and FFT analysis of the inductor current to visualise amplitudes of the inductor current harmonics.

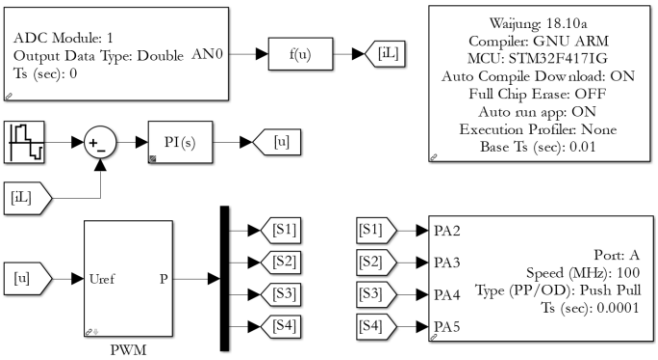

Figure 16: Simulink diagram to deploy the SPWM method on the KIT STM32F407 DISCOVERY.

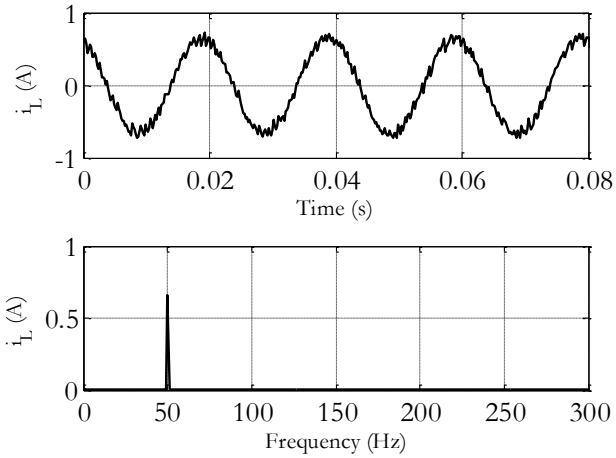

Figure 17: Waveform and FFT of the inductor current (the SPWM method).

4.2. Current Control Using the Hysteresis Method

Figure 18 is a Simulink diagram to deploy the hysteresis control method on the KIT STM32F407 DISCOVERY. The control method needs the measurement of the inductor current. When the error between the reference and measured currents crosses either the positive or negative boundary of the hysteresis band, a significant change in the output of the controller occurs. Therefore, the controller can quickly react to any deviation from the reference current, which is the reason for the high gain behaviour of the controller.

Compared to the SPWM method, the hysteresis method does not require the generation of PWM, and it is also quite simple to be implemented and belongs to non-linear control techniques. In this case, waveforms and RMS values of the inverter output voltage and the inductor current were also acquired using the NI-6009 DAQ device for an offline analysis using MATLAB. Figure 19 is waveform and FFT analysis of the inductor current.

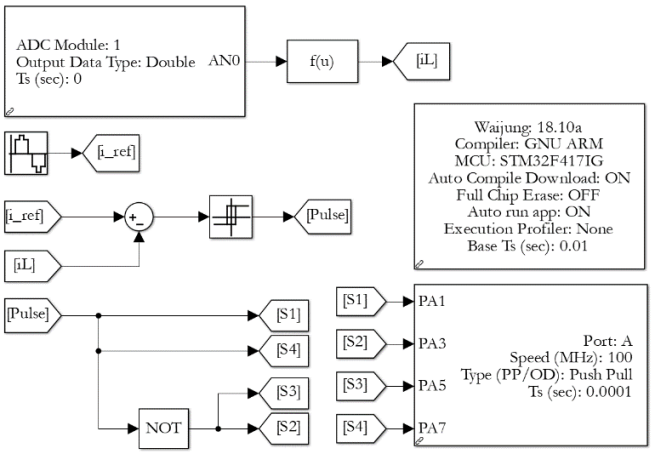

Figure 18: Simulink diagram to deploy the hysteresis control method on the KIT STM32F407 DISCOVERY.

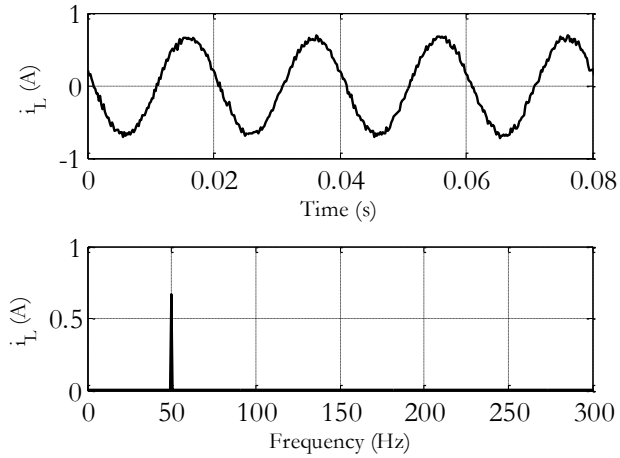

Figure 19: Waveform and FFT analysis of the inductor current (the hysteresis method).

4.3. Current Control Using the MPC Method

Figure 20 is a Simulink diagram to deploy the MPC method on the KIT STM32F4 DISCOVERY. Figure 21 is waveform and FFT analysis of the inductor current.

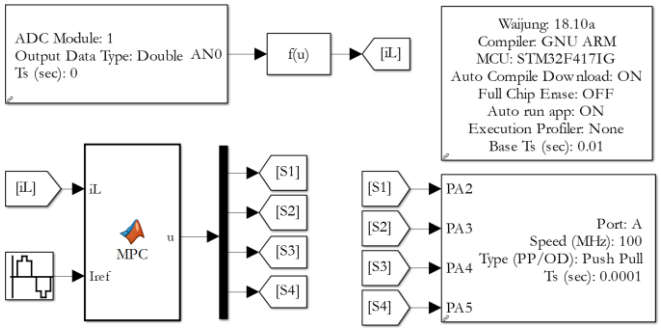

Figure 20: Simulink diagram to deploy the MPC method on the KIT STM32F407 DISCOVERY.

The MATLAB function of the MPC controller in Simulink has the following form:

```
function pulse = MPC(i,i_ref)
R = 210;
L = 0.6667;
Vdc = 320;
Ts = 1e-4;
Sa_opt = 0;
Sb_opt = 0;
g_opt = inf;
for Sa = 0:1
   for Sb = 0:1
      Vab = Vdc*(Sa - Sb);
      i_1 = L/(L + R*Ts)*i + Ts/(L + R*Ts)*Vab ;
      g = abs(i_ref - i_1);
      if (g < g_opt)
         Sa_opt = Sa;
         Sb_opt = Sb;
         g_opt = g;
      end
   end
end
Sa = Sa_opt;
Sb = Sb_opt;
pulse = [Sa; not(Sa); Sb; not(Sb)];
```

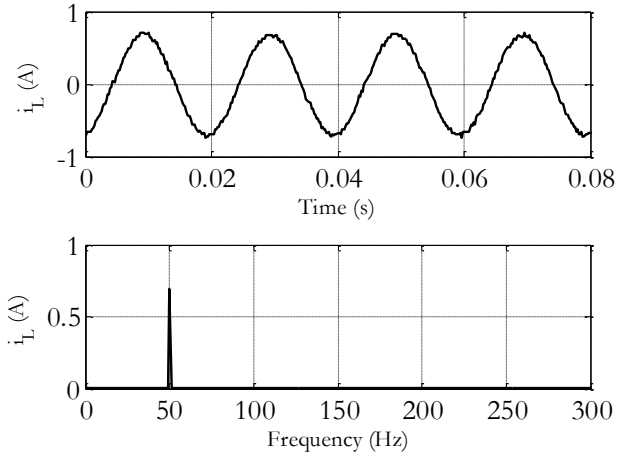

Figure 21: Waveform and FFT analysis of the load current (the MPC method).

Table 2 shows a comparison of three control methods of the output current of the inverter. In general, three control methods can result in sinusoidal waves with very low THD. However, the MPC method can give the lowest THD with a percentage of 0.9825.

Table 2: THD of the inductor current corresponding to three control methods.

Control Method	THD (%)
SPWM	5.0378
Hysteresis	1.3650
MPC	0.9825

4.4. Voltage Control Using the MPC Method

In UPS applications, the capacitor voltage needs to be controlled so that it can have a nearly sinusoidal wave. In this case, the desired amplitude of the capacitor voltage is 100 (V). Figure 22 is a Simulink diagram to deploy the MPC method on the KIT STM32F407 DISCOVERY. Figure 23 shows waveform and FFT analysis of the capacitor voltage.

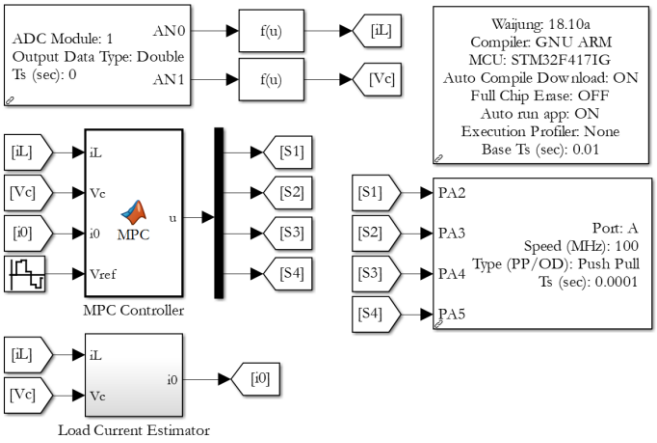

Figure 22: Simulink diagram to deploy the MPC method on the KIT STM32F4 DISCOVERY.

The MATLAB function of the MPC controller has the following form:

```
function u = MPC(iL,Vc,i0,Vref)
L = 0.6667;
C = 8e-6;
Vdc = 260;
Ts = 1e-3;
Sa_opt = 0;
Sb_opt = 0;
g_opt = inf;
for Sa = 0:1
   for Sb = 0:1
      Vab = Vdc*(Sa - Sb);
      iL_1 = iL + Ts/L*(Vab - Vc);
      Vc_1 = Vc + Ts/C*(iL_1 - i0);
      g = (Vref - Vc_1)^2;
      if (g < g_opt)
         Sa_opt = Sa;
         Sb_opt = Sb;
         g_opt = g;
      end
   end
end
Sa = Sa_opt;
Sb = Sb_opt;
u = [Sa; not(Sa); Sb; not(Sb)];
```

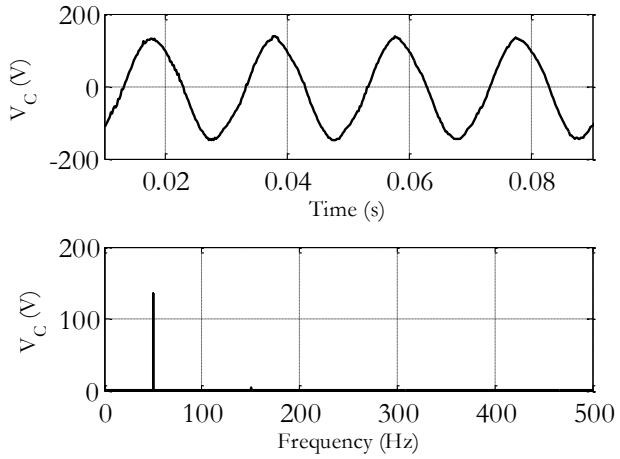

Figure 23: Waveform and FFT analysis of the capacitor voltage.

5. Conclusion

This study focuses on the exploration of the KIT STM32F407 DISCOVERY, which is computationally fast and has also a reasonable price. With the use of the Waijung library, the KIT STM32F407 DISCOVERY can conveniently allow users to directly transfer proposed control algorithms from the Simulink environment to the KIT STM32F407 DISCOVERY. In addition, the proposed control algorithms for the single-phase voltage-source inverter can be easily verified by Simulink-based simulation tasks before they can be deployed on the KIT STM32F407 DISCOVERY. The study performs three control methods for the current-controlled single-phase inverter. The output voltage control of the single-phase UPS is also mentioned in detail. According to the experimental results obtained, the performance of the inverters controlled by the FCS-MPC method can outperform the performance of the inverter controlled by conventional control methods. The future work of this study is to explore the KIT STM32F407 DISCOVERY to control current and voltage the three-phase voltage-source inverter and other types of power converters using the FCS-MPC algorithm.

References

[1] Yongheng Yang, Keliang Zhou, Frede Blaabjerg, "Current Harmonics From Single-Phase Grid-Connected Inverters—Examination and Suppression", *IEEE Journal of Emerging and Selected Topics in Power Electronics*, vol. 4, no. 1, pp. 221-233, Mar. 2016, doi: 10.1109/JESTPE.2015.2504845.

[2] Guo-rong Zhu, Haoran Wang, Biao Liang, Siew-Chong Tan, Jin Jiang, "Enhanced Single-Phase Full-Bridge Inverter With Minimal Low-Frequency Current Ripple", *IEEE Transactions on Industrial Electronics*, vol. 63, no. 2, pp. 937-943, Oct. 2015, doi: 10.1109/TIE.2015.2491881.

[3] Shuang Xu, Liuchen Chang, Riming Shao, "Single-Phase Voltage Source Inverter With Voltage Boosting and Power Decoupling Capabilities", *IEEE Journal of Emerging and Selected Topics in Power Electronics*, vol. 8, no. 3, pp. 2977-2988, Sep. 2020, doi: 10.1109/JESTPE.2019.2936136.

[4] Shungang Xu, Jinping Wang, Jianping Xu, "A Current Decoupling Parallel Control Strategy of Single-Phase Inverter With Voltage and Current Dual Closed-Loop Feedback", *IEEE Transactions on Industrial Electronics*, vol. 60, no. 4, pp. 1306-1313, Apr. 2013, doi: 10.1109/TIE.2011.2161660.

[5] Moria Elkayam; Alon Kuperman, "Optimized Design of Multiresonant AC Current Regulators for Single-Phase Grid-Connected Photovoltaic Inverters", *IEEE Journal of Photovoltaics*, vol. 9, no. 6, pp. 1815-1818, Sep. 2019, doi: 10.1109/JPHOTOV.2019.2937386.

[6] Mohammad Parvez, Mohamad Fathi Mohamad Elias, Nasrudin Abd Rahim, Frede Blaabjerg, Derek Abbott, Said F. Al-Sarawi, "Comparative Study of Discrete PI and PR Controls for Single-Phase UPS Inverter", *IEEE Access*, vol. 8, Jan 2020, pp. 45584-45595, doi: 10.1109/ACCESS.2020.2964603.

[7] Jeyraj Selvaraj, Nasrudin A. Rahim, "Multilevel Inverter For Grid-Connected PV System Employing Digital PI Controller", *IEEE Transactions on Industrial Electronics*, vol. 56, no. 1, Jan 2009, pp. 149- 158, doi: 10.1109/TIE.2008.928116.

[8] P. Mattavelli, "An improved deadbeat control for UPS using disturbance observers", *IEEE Transactions on Industrial Electronics*, vol. 52, no. 1, Feb 2005, pp. 206-212, doi: 10.1109/TIE.2004.837912.

[9] F. Zare, G. Ledwich, "A Hysteresis Current Control for Single-Phase Multilevel Voltage Source Inverters: PLD Implementation", *IEEE Transactions on Power Electronics*, vol. 17, no. 5, Sep 2002, pp. 731–738, doi: 10.1109/TPEL.2002.802192.

[10] Heng Deng, Ramesh Oruganti, Dipti Srinivasan, "Analysis and Design of Iterative Learning Control Strategies for UPS Inverters", *IEEE Transactions on Industrial Electronics*, vol. 54, no. 3, Jun 2007, pp. 1739 –1751, May. 2007, doi: 10.1109/TIE.2007.894701.

[11] Tsang-Li Tai, Jian-Shiang Chen, "UPS inverter design using discrete-time sliding-mode control scheme", *IEEE Transactions on Industrial Electronics*, vol. 49, no. 1, pp. 67–75, Feb. 2002, doi: 10.1109/41.982250.

[12] P. Ubare and D. N. . Sonawane, "Performance Assessment of the BLDC Motor in EV Drives using Nonlinear Model Predictive Control", *Eng. Technol. Appl. Sci. Res.*, vol. 12, no. 4, pp. 8901–8909, Aug. 2022, doi: https://doi.org/10.48084/etasr.4976.

[13] S. Masoumi Kazraji, M. R. Feyzi, M. B. Bannae Sharifian, and S. Tohidi, "Fuzzy Predictive Force Control (FPFC) for Speed Sensorless Control of Single-side Linear Induction Motor", *Eng. Technol. Appl. Sci. Res.*, vol. 7, no. 6, pp. 2132–2138, Dec. 2017, doi: https://doi.org/10.48084/etasr.1591.

[14] T. A. Trivedi, R. Jadeja, and P. Bhatt, "A Review on Direct Power Control for Applications to Grid Connected PWM Converters", *Eng. Technol. Appl. Sci. Res.*, vol. 5, no. 4, pp. 841–849, Aug. 2015, doi: https://doi.org/10.48084/etasr.544.

[15] H. Bassi and Y. A. Mobarak, "State-Space Modeling and Performance Analysis of Variable-Speed Wind Turbine Based on a Model Predictive Control Approach", *Eng. Technol. Appl. Sci. Res.*, vol. 7, no. 2, pp. 1436–1443, Apr. 2017, doi: https://doi.org/10.48084/etasr.1015.

[16] Jos Rodriguez, Jorge Pontt, Csar A. Silva, Pablo Correa, Pablo Lezana, Patricio Cortes, Ulrich Ammann, "Predictive Current Control of a Voltage Source Inverter", *IEEE Transactions on Industrial Electronics*, vol. 54, no. 1, pp. 495–503, Feb 2007, doi: 10.1109/TIE.2006.888802.

[17] Samir Kouro, Patricio Cortés, René Vargas, Ulrich Ammann, José Rodriguez, "Model Predictive Control–A Simple and Powerful Method to Control Power Converters", *IEEE Transactions on Industrial Electronics*, vol. 56, no. 6, pp. 1826–1838, Nov 2008, doi: 10.1109/TIE.2008.2008349.

[18] The Waijung Blockset, the legacy Simulink Embedded Target for the STM32F4: https://www.aimagin.com/en/